



# Hepatocellular carcinoma detection in liver cirrhosis: diagnostic performance of contrast-enhanced CT vs. MRI with extracellular contrast vs. gadoxetic acid

Sahar Semaan<sup>1,2</sup> · Naik Vietti Violi<sup>2,3</sup> · Sara Lewis<sup>1,2</sup> · Manjil Chatterji<sup>1</sup> · Christopher Song<sup>1</sup> · Cecilia Besa<sup>2,4</sup> · James S. Babb<sup>5</sup> · M. Isabel Fiel<sup>6</sup> · Myron Schwartz<sup>7</sup> · Swan Thung<sup>6</sup> · Claude B. Sirlin<sup>8</sup> · Bachir Taouli<sup>1,2</sup>

Received: 14 June 2019 / Revised: 7 August 2019 / Accepted: 13 September 2019 / Published online: 31 October 2019  
© European Society of Radiology 2019

## Abstract

**Objectives** To evaluate the diagnostic performance of contrast-enhanced CT vs. MRI with extracellular contrast agents (EC-MRI) vs. MRI with gadoxetic acid (EOB-MRI) for HCC detection in patients with liver cirrhosis using liver explant as the reference. The additional value of hepatobiliary phase (HBP) post Gadoxetic acid was also assessed.

**Methods** Two-hundred seventy-seven consecutive patients who underwent liver transplantation over a 9 year period and imaging within 90 days of were retrospectively included. Imaging consisted in CT ( $n = 100$ ), EC-MRI ( $n = 77$ ) and EOB-MRI ( $n = 100$ ), the latter subdivided into dynamic EOB-MRI and full EOB-MRI (dynamic+HBP). Three radiologists retrospectively categorized lesions  $\geq 1$  cm using the LI-RADSv2017 algorithm. Dynamic EOB-MRI was re-evaluated with the addition of HBP. Results were correlated with explant pathology.

**Results** Pathology demonstrated 265 HCCs (mean size  $2.1 \pm 1.4$  cm) in 177 patients. Per-patient sensitivities were 86.3% for CT, 89.5% for EC-MRI, 92.8% for dynamic EOB-MRI and 95.2% for full EOB-MRI (pooled reader data), with a significant difference between CT and dynamic/full EOB-MRI ( $p = 0.032/0.002$ ), and between EC-MRI and full EOB-MRI ( $p = 0.047$ ). Per-lesion sensitivities for CT, EC-MRI, dynamic EOB-MRI and full EOB-MRI were 59.5%, 78.5%, 69.7% and 76.8%, respectively, with a significant difference between MRI groups and CT ( $p$ -range: 0.001–0.04), and no difference between EC-MRI and dynamic EOB-MRI ( $p = 0.949$ ). For HCCs 1–1.9 cm, sensitivities were 34.4%, 64.6%, 57.3% and 67.3%, respectively, with all MRI groups significantly superior to CT ( $p \leq 0.01$ ) and full EOB-MRI superior to dynamic EOB-MRI ( $p = 0.002$ ).

**Conclusions** EOB-MRI outperforms CT and EC-MRI for per-patient HCC detection sensitivity, and is equivalent to EC-MRI for per-lesion sensitivity. MRI methods outperform CT for detection of HCCs 1–1.9 cm.

Sahar Semaan and Naik Vietti Violi are co-first authors.

**Electronic supplementary material** The online version of this article (<https://doi.org/10.1007/s00330-019-06458-4>) contains supplementary material, which is available to authorized users.

✉ Bachir Taouli  
bachir.taouli@mountsinai.org

<sup>1</sup> Department of Radiology, Body MRI, Icahn School of Medicine at Mount Sinai, One Gustave L. Levy Place, 1470 Madison Avenue, New York, NY 10029, USA

<sup>2</sup> Translational and Molecular Imaging Institute, Icahn School of Medicine at Mount Sinai, One Gustave L. Levy Place, 1470 Madison Avenue, New York, NY 10029, USA

<sup>3</sup> Department of Radiology, Lausanne University Hospital, Rue du Bugnon 46, 1011 Lausanne, Switzerland

<sup>4</sup> Department of Radiology, School of Medicine, Pontificia Universidad Católica de Chile, Avenida Libertador Bernardo O'Higgins 340, 8331150 Santiago, Chile

<sup>5</sup> Department of Radiology, New York University Langone Medical Center, 333 E 38th Street, New York, NY 10016, USA

<sup>6</sup> Department of Pathology, Icahn School of Medicine at Mount Sinai, One Gustave L. Levy Place, New York, NY 10029, USA

<sup>7</sup> Recanati/Miller Transplantation Institute, Icahn School of Medicine at Mount Sinai, One Gustave L. Levy Place, New York, NY, USA

<sup>8</sup> Liver Imaging Group, Department of Radiology, UC San Diego Medical Center, 200 West Arbor Drive, San Diego, CA, USA

## Key points

- MRI is superior to CT for HCC detection in patients with liver cirrhosis.
- EOB-MRI outperforms CT and MRI using extracellular contrast agents (EC-MRI) for per-patient HCC detection sensitivity, and is equivalent to EC-MRI for per-lesion sensitivity.
- The addition of hepatobiliary phase images improves HCC detection when using gadoxetic acid.

**Keywords** Liver neoplasms · Magnetic resonance imaging · Contrast media · Tomography, spiral computed

## Abbreviations

CT	Computed tomography
DWI	Diffusion-weighted imaging
EC-MRI	Extracellular gadolinium based contrast-enhanced MRI
EOB-MRI	Gadoxetic acid-enhanced MRI
FP	False positive
GBCAs	Gadolinium based contrast agents
HBP	Hepatobiliary phase
LI-RADS	Liver imaging reporting and data system
NPV	Negative predictive value
PPV	Positive predictive value
TN	True negative
TP	True positive
UNOS	United network for organ sharing

## Introduction

Hepatocellular carcinoma (HCC) is the second leading cause of cancer-related death worldwide [1]. HCC is typically diagnosed using dynamic contrast-enhanced CT or MRI. The imaging diagnosis of HCC typically relies on enhancement characteristics such as hyperenhancement during the arterial phase relative to the surrounding liver parenchyma and washout in portal venous or delayed venous phases post-contrast on CT and MRI [2]. While CT has the advantage of being widely available and quicker, it exposes patients to ionizing radiation. On the other hand, by combining multiple pulse sequences, MRI offers better tissue characterization, which aids in HCC diagnosis [3]. The sensitivity for HCC detection using CT has been reported to vary between 50%–80%, compared to 52%–93% for MRI [4–13], with superiority of MRI for detecting small HCCs [3, 9, 13].

Various gadolinium-based contrast agents (GBCAs) can be utilized when performing liver MRI, including extracellular (EC) agents and liver-specific agents (Gadobenate Dimeglumine and Gadoxetic acid EOB-DTPA) [6, 14–16]. Even if EOB-MRI demonstrates high sensitivity for HCC detection with the addition of T1-weighted imaging obtained during the hepatobiliary phase (HBP) (92%), there is no clear demonstrated superiority of EOB-MRI over EC-MRI in terms of HCC detection [11].

Prior studies have assessed the diagnostic performance of CT and EC-MRI using liver explant pathology as the

reference, with diagnostic per-lesion sensitivity for HCC detection ranging between 46%–98% for CT [17, 18] and 77.8%–100% for EC-MRI [6, 19, 20]. The published evidence for EOB-MRI in comparison with liver explant pathology is small, with 3 studies demonstrating per-lesion sensitivity ranging between 44.8%–94.6% [21–23]. It is generally accepted that EC-MRI is superior to CT for detection of small HCCs [10, 24]. Although there have been several studies comparing the diagnostic performance of CT or EC-MRI to EOB-MRI [4, 7–9, 25–27], the incremental value of EOB-MRI for HCC detection with explant pathology needs to be established. Current North American and European guidelines recommend either CT or MRI without specifying the type of gadolinium based contrast to be used for HCC diagnosis and staging before transplantation, due to lack of published evidence and absence of consensus in favor of one technique [28, 29]. Thus, the comparison of CT, EC-MRI and EOB-MRI is warranted to establish the optimal method for HCC diagnosis.

The main objective of our study was to compare the diagnostic performance of CT, EC-MRI and EOB-MRI for HCC diagnosis in pre-transplant cirrhotic patients, using liver explant as the reference. A secondary objective was to evaluate the added value of HBP for HCC detection when using Gadoxetic acid.

## Materials and methods

### Patients

This single-center HIPAA compliant retrospective study was approved by the local IRB, with a waiver for informed consent. All consecutive patients who underwent liver transplantation and had undergone CT or MRI, using either EC-GBCA or gadoxetic acid between November 2006 and October 2015 were identified through the institutional liver transplant database. Inclusion criteria were: a) Adult patients with liver cirrhosis that underwent liver transplantation over a period of 9 years, b) CT or MRI performed with an adequate technique and quality within 90 days prior to liver transplantation. Exclusion criteria were: a) Interval treatment between imaging and transplantation, b) Suboptimal image quality (exams with major breathing artifacts) or single-phase CT. Among 534 patients, 277 patients were retained for the study (M/F: 199/

78, mean age  $60 \pm 11$  y, range:23-77y). Patients were divided into three groups based on the type of pre-transplant imaging modality performed: CT ( $n = 100$ ), EC-MRI ( $n = 77$ ) and EOB-MRI ( $n = 100$ ) (Fig. 1). The choice of imaging modality (CT or MRI) was based on the physician's preference. No patient had multiple imaging modalities within 90 days to transplantation. Consequently, each patient was included only in one study group.

All patients had liver cirrhosis, ranging in etiology as follows: chronic hepatitis C ( $n = 154$ ), alcohol abuse ( $n = 29$ ), chronic hepatitis B ( $n = 24$ ), primary biliary cirrhosis ( $n = 16$ ), nonalcoholic steatohepatitis ( $n = 21$ ), autoimmune hepatitis ( $n = 13$ ), primary sclerosing cholangitis ( $n = 12$ ) and cryptogenic cirrhosis ( $n = 8$ ). All patients were transplanted based on United Network for Organ Sharing (UNOS) liver allocation selection criteria [2], including 157 patients (57%) that received locoregional therapies for HCC downstaging.

## Imaging

All imaging studies were performed with state-of-the-art systems, using standard liver dedicated protocol. Details on the imaging systems and protocols are provided in [supplemental material](#).

## Image analysis

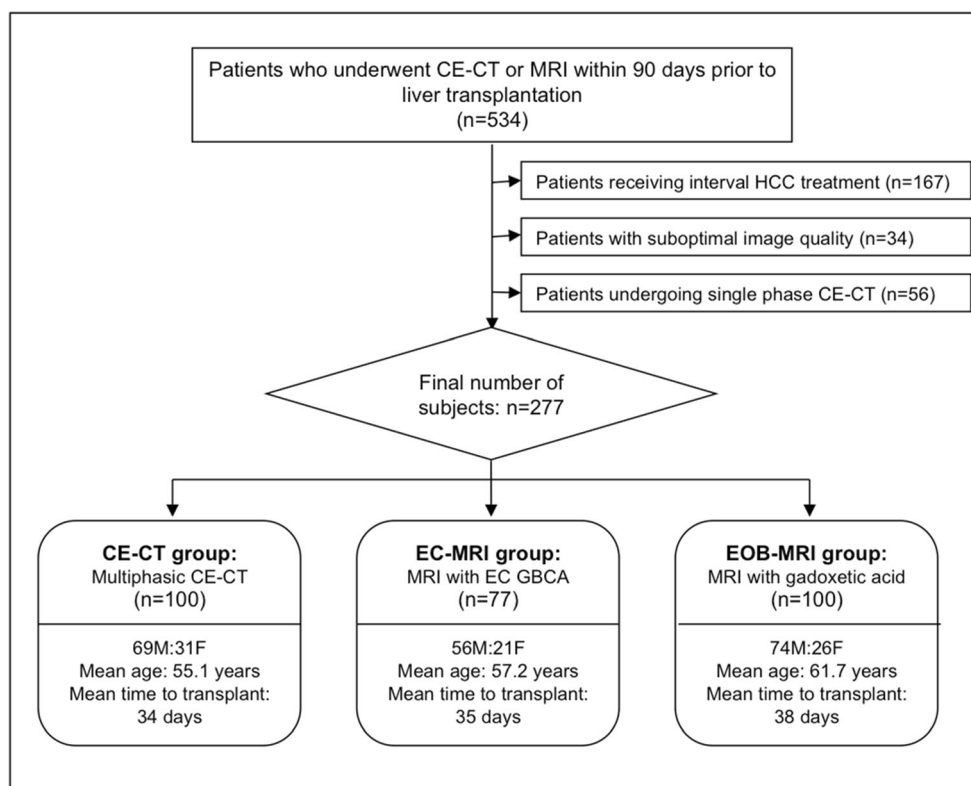
Three radiologists (CS, reader 1; SL, reader 2, and MC, reader 3) with 1, 7, and 8 years of experience in abdominal imaging,

respectively, independently reviewed the images on a picture archiving and communication system (PACS). Exams were reviewed in a different random order (including the imaging modality) but if an exam contained multiple lesions all lesions were scored in the same reading session. The readers were asked to record all hepatic observations measuring  $\geq 1$  cm (excluding cysts and hemangiomas), with mention of lesion size and Couinaud segment location.

The readers categorized lesions using the Liver Imaging Reporting and Data System (LI-RADS) v2017 diagnostic algorithm relying on dynamic contrast-enhanced sequences [30]. A lesion was diagnosed as HCC if it was categorized as LI-RADS 5. Washout and capsule enhancement were assessed on portal venous or equilibrium/transitional phases for the EC-MRI group and on portal venous phase only for the EOB-MRI group. The readers were blinded to all radiological and pathological clinical reports and to treatment history. As diffusion-weighted imaging (DWI) was made systematically available on routine MRI protocols only after 2011, it was not assessed in this study.

The images from the EOB-MRI group were reviewed in a second reading session at least 6 weeks after the initial assessment, to minimize recall bias. The readers were asked to reassess all lesions  $\geq 1$  cm, using dynamic contrast-enhanced characteristics with the addition HBP sequence, and assign appropriate LI-RADS scores, without the information from the first reading. Hypointensity on HBP was used as an ancillary finding according to the LI-RADSv2017 diagnostic

**Fig. 1** Flow chart of patient population. Abbreviations: CE-CT: contrast-enhanced computed tomography, EC-MRI: extracellular gadolinium based contrast-enhanced MRI, EOB-MRI: gadoxetic acid-enhanced MRI.



algorithm in the hope of improving lesion detection. Any finding detected on this sequence was reported by the reader and analyzed back on dynamic contrast-enhanced in order to apply a LI-RADS score.

## Reference standard

The study coordinator (SS) reviewed the images and correlated the lesions recorded on imaging with the explant pathologic findings, based on lesion size and segment location. Cholangiocarcinoma and mixed HCC-cholangiocarcinoma tumors were excluded from the analysis. Only viable HCCs  $\geq 1$  cm on pathology were included in the study. Lesions scored LI-RADS 1–4 and LI-RADS M were considered negative for HCC. Completely necrotic tumors were excluded from analysis. Lesion size on pathology was used to define sub-groups of analysis: 1–1.9 cm and  $\geq 2$  cm. On a lesion-basis, true positive (TP) was defined as a lesion scored LI-RADS 5 with corresponding HCC in the same segment location at pathology. True negative (TN) was defined when no lesion was reported or scored LI-RADS 5 and no HCC was found in the same segment location at pathology. False positive (FP) was defined when a lesion was scored LI-RADS 5 and no HCC was found in the same segment location at pathology. False negative (FN) was defined when an HCC was found at pathology and no lesion was scored LI-RADS 5 in the same segment location. On a patient-basis, TP was defined when at least one TP lesion was found. TN was defined when no lesion was found or all observations were considered TN. FP was defined when no HCC was found at pathology and at least one FP lesion was recorded. FN was defined when at least one HCC was found at pathology and no lesion was considered TP.

## Statistical analysis

All statistical tests were conducted at the two-sided 5% significance level using SAS version 9.3 (SAS Institute). Logistic regression for correlated data was used to assess and compare the imaging methods in terms of per-patient and per-lesion diagnostic accuracy for the detection of HCC using explant pathology used as reference standard. Per-patient and per-lesion analyses are important for patient classification and liver transplant eligibility [2]. For the per-lesion analysis, an indicator variable identifying the lesion associated with each observation was included in the model as a blocking factor so that methods could be compared on a per-lesion basis and results then pooled over lesions. Per-lesion and per-patient sensitivity, specificity, positive predictive value (PPV), negative predictive value (NPV) and accuracy were calculated for each modality, and the performance characteristics of the imaging modalities were compared. The per-lesion analysis for HCC detection were first conducted using data from all

lesions regardless of size and then stratified according to lesion size at pathology (1–1.9 cm or  $\geq 2$  cm). Inter-reader agreement for HCC detection was assessed using kappa ( $\kappa$ ) coefficients.

## Results

### Histopathologic results

A total of 376 HCCs were identified in 177 patients. There were 5 patients with 5 non-HCC malignancy (1 cholangiocarcinoma and 4 mixed HCC-cholangiocarcinomas). These patients were not excluded (as they also had HCC), however the 5 non-HCC malignant lesions were excluded from per-lesion analysis. Out of 277 patients, 100 (36.1%) patients had no HCC, 84 (30.3%) patients had 1 HCC, 39 (14.1%) patients had 2 HCCs, 24 (8.7%) patients had 3 HCCs and 30 (10.8%) patients had more than 3 HCCs. Out of these tumors, 265 HCCs were viable ( $n = 72$  in CT group,  $n = 61$  in EC-MRI group, and  $n = 132$  in EOB-MRI group) and 106 HCCs were completely necrotic ( $n = 40$  in CT group,  $n = 11$  in EC-MRI group, and  $n = 55$  in EOB-MRI group). Differentiation of viable tumors was as follows: 85 well differentiated, 163 moderately differentiated, and 17 poorly differentiated. The mean size of the viable lesions was 2.1 cm  $\pm$  1.4 cm, ranging from 1.0–9.1 cm. When stratified according to size, 158 HCCs were 1–1.9 cm ( $n = 46$  in CT group,  $n = 30$  in EC-MRI group, and  $n = 82$  in EOB-MRI group) and 107 HCCs measured  $\geq 2$  cm ( $n = 26$  in CT group,  $n = 31$  in EC-MRI group, and  $n = 50$  in EOB-MRI group).

### Interobserver agreement

There was substantial agreement among readers for LI-RADS 5 categorization, with concordance rates of 90.7% for the CT group ( $\kappa = 0.810$ ), 95.2% for the EC-MRI group ( $\kappa = 0.905$ ), 88.7% for the dynamic EOB-MRI group ( $\kappa = 0.754$ ), and 89.0% for the full EOB-MRI group ( $\kappa = 0.735$ ).

### HCC detection per patient

There was no significant difference in the specificity, PPV or accuracy between the groups when pooling all three readers together (Table 1). However, dynamic EOB-MRI was found to be superior to CT in terms of sensitivity ( $p = 0.032$ ) and NPV ( $p = 0.043$ ). There was no significant difference between dynamic EOB-MRI and EC-MRI in terms of sensitivity ( $p = 0.292$ ), however full EOB-MRI had a significantly higher sensitivity than CT ( $p = 0.002$ ) and EC-MRI ( $p = 0.047$ ).

**Table 1** Per-patient diagnostic performance for each modality for HCC detection with 95% confidence intervals

Group		Sensitivity	Specificity	PPV	NPV	Accuracy
Reader 1	CT	83.9% (71.7–92.4%)	97.7% (88.0–99.9%)	97.9% (88.9–99.9%)	82.7% (69.7–91.8%)	90.0% (92.4–95.1%)
	EC-MRI	84.2% (68.7–94.0%)	100% (92.1–100%)	100% (90.5–100%)	86.7% (73.2–94.9%)	92.2% (83.8–97.1%)
	Dynamic EOB-MRI	91.6% (83.4–96.5%)	94.2% (71.3–99.9%)	98.7% (93.0–100%)	69.6% (47.1–86.8%)	92.0% (84.8–96.5%)
	Full EOB-MRI	92.8% (84.9–97.3%)	94.1% (71.3–99.9%)	98.7% (93.1–100%)	72.7% (49.8–89.3%)	93.0% (86.1–97.1%)
Reader 2	CT	89.3% (78.1–96.0%)	95.5% (84.5–99.4%)	96.2% (86.8–99.5%)	87.5% (74.8–95.3%)	92.0% (84.8–96.5%)
	EC-MRI	92.1% (78.6–98.3%)	97.4% (86.5–99.9%)	97.2% (85.5–99.9%)	92.7% (80.1–98.5%)	94.8% (87.2–98.6%)
	Dynamic EOB-MRI	94.0% (86.5–98.0%)	94.1% (71.3–99.9%)	98.7% (93.1–100%)	76.2% (52.8–91.8%)	94.0% (87.4–97.8%)
	Full EOB-MRI	96.4% (89.8–99.2%)	94.1% (71.3–99.9%)	98.8% (93.3–100%)	84.2% (60.4–96.6%)	96.0% (90.1–98.9%)
Reader 3	CT	85.7% (73.8–93.6%)	100% (92.8–100%)	100% (93.4–100%)	84.6% (71.9–93.1%)	92.0% (84.8–96.5%)
	EC-MRI	92.1% (78.6–98.3%)	100% (92.1–100%)	100% (91.3–100%)	92.9% (80.5–98.5%)	96.1% (89.0–99.2%)
	Dynamic EOB-MRI	92.8% (84.9–97.3%)	100% (81.6–100%)	100% (95.4–100%)	73.9% (51.6–89.8%)	94.0% (87.4–97.8%)
	Full EOB-MRI	96.4% (89.8–99.2%)	94.1% (71.3–99.9%)	98.8% (93.3–100%)	84.2% (60.4–96.6%)	96.0% (90.1–98.9%)
Pooled reader data	CT	86.3% (80.2–91.1%)	97.7% (93.5–99.5%)	98.0% (94.2–99.6%)	84.9% (78.2–90.2%)	91.3% (97.6–94.3%)
	EC-MRI	89.5% (82.3–94.4%)	97.7% (95.3–100%)	99.0% (94.7–100%)	90.6% (84.2–95.1%)	94.4% (90.6–97.0%)
	Dynamic EOB-MRI	92.8% (88.8–95.7%)	96.1% (86.5–99.5%)	96.1% (93.8–100%)	73.1% (60.9–83.2%)	93.3% (89.9–95.9%)
	Full EOB-MRI	95.2% (91.7–97.5%)	94.1% (71.3–99.9%)	98.8% (96.4–99.7%)	80.0% (67.7–89.2%)	95.0% (91.9–97.2%)
	<i>p</i> (CT vs. EC-MRI)	0.430	0.393	0.520	0.150	0.187
	<i>p</i> (CT vs. Dynamic EOB-MRI)	0.032	0.545	0.343	0.043	0.359
	<i>p</i> (CT vs. Full EOB-MRI)	0.002	0.236	0.551	0.391	0.079
	<i>p</i> (EC-MRI vs. Dynamic EOB-MRI)	0.292	0.209	0.920	0.002	0.623
	<i>p</i> (EC-MRI vs. Full EOB-MRI)	0.047	0.090	0.826	0.046	0.749
	<i>p</i> (Dynamic EOB-MRI vs. Full EOB-MRI)	0.262	0.649	0.679	0.365	0.385

PPV: positive predictive value, NPV: negative predictive value, CE-CT: contrast-enhanced computed tomography, EC-MRI: extracellular gadolinium based contrast-enhanced MRI, EOB-MRI: gadoxetic acid-enhanced MRI

### HCC detection per lesion

Both MRI techniques had significantly higher per-lesion sensitivity for HCC than CT (Table 2). There was no significant difference in the sensitivity for HCC between EC-MRI and dynamic EOB-MRI ( $p = 0.949$ ). Despite this, the addition of HBP significantly improved the sensitivity of EOB-MRI for HCC detection ( $p = 0.006$ ). There were no significant differences in specificity or PPV between the imaging modalities. Examples of HCCs with CT, EOB-MRI and EC-MRI are shown in Figs. 2–4.

**Per-Lesion Sensitivity Stratified by Tumor Size** There was no significant difference in sensitivity for HCCs  $\geq 2$  cm between modalities for any individual reader or when pooling readers together, with sensitivity ranging between 83.9% and 93.8% for the pooled reader data (Table 3). For HCCs 1–1.9 cm, the sensitivity of MRI using either type of GBCA (64.6% with EC-MRI and 67.3% for full EOB-MRI using pooled reader data) was significantly higher than CT (34.4% sensitivity using pooled reader data,  $p = 0.012$  and 0.003, respectively). There was no significant difference between the EC-

**Table 2** Per-lesion sensitivity for each modality for HCC detection with 95% confidence intervals

Group		Sensitivity	Specificity	PPV	Accuracy
Reader 1	CT	57.1% (47.5–66.5%)	97.8% (88.2–99.9%)	98.5% (91.7–100%)	68.8% (60.9–75.9%)
	EC-MRI	76.7% (65.5–85.8%)	100% (92.1–100%)	100% (94.2–100%)	84.8% (76.8–90.9%)
	Dynamic EOB-MRI	64.2% (56.9–71.0%)	84.2% (60.4–96.6%)	97.6% (93.0–99.5%)	66.0% (59.1–72.5%)
	Full EOB-MRI	70.6% (63.5–77.0%)	94.7% (74.0–99.9%)	99.2% (95.9–100%)	72.8% (66.2–78.8%)
Reader 2	CT	63.4% (53.8–72.3%)	93.3% (81.7–98.6%)	95.9% (88.6–99.2%)	70.1% (64.3–78.8%)
	EC-MRI	79.5% (68.4–88.0%)	97.4% (86.5–99.9%)	98.3% (90.9–100%)	86.6% (77.8–91.6%)
	Dynamic EOB-MRI	73.8% (66.9–79.9%)	94.7% (74.0–99.9%)	99.3% (96.1–100%)	73.8% (69.3–81.4%)
	Full EOB-MRI	80.7% (74.4–86.1%)	89.5% (66.9–98.7%)	98.7% (95.4–99.8%)	80.1% (75.6–86.6%)
Reader 3	CT	58.0% (48.3–67.3%)	100% (93.0–100%)	100% (94.5–100%)	70.1% (62.3–77.1%)
	EC-MRI	79.5% (68.4–88.0%)	100% (92.1–100%)	100% (94.3–100%)	86.6% (78.9–92.3%)
	Dynamic EOB-MRI	71.1% (64.1–77.5%)	100% (83.7–100%)	100% (97.4–100%)	73.8% (67.2–79.7%)
	Full EOB-MRI	79.1% (72.6–84.7%)	89.5% (66.9–98.7%)	98.7% (95.3–99.8%)	80.1% (74.0–85.3%)
Pooled reader data	CT	59.5% (54.1–64.8%)	97.0% (92.6–99.2%)	98.0% (95.1–99.5%)	70.3% (65.9–74.4%)
	EC-MRI	78.5% (72.5–83.8%)	99.1% (95.3–100%)	99.4% (96.8–100%)	85.7% (81.5–89.3%)
	Dynamic EOB-MRI	69.7% (65.7–73.5%)	93.0% (83.0–98.1%)	99.0% (97.4–99.7%)	71.8% (68.1–75.4%)
	Full EOB-MRI	76.8% (73.1–80.3%)	91.2% (80.7–97.1%)	98.9% (97.3–99.6%)	78.2% (74.7–81.4%)
	<i>p</i> (CT vs. EC-MRI)	0.040	0.255	0.384	0.019
	<i>p</i> (CT vs. Dynamic EOB-MRI)	0.013	0.249	0.406	0.626
	<i>p</i> (CT vs. Full EOB-MRI)	0.001	0.201	0.446	0.085
	<i>p</i> (EC-MRI vs. Dynamic EOB-MRI)	0.949	0.063	0.829	0.049
	<i>p</i> (EC-MRI vs. Full EOB-MRI)	0.280	0.053	0.826	0.483
	<i>p</i> (Dynamic EOB-MRI vs. Full EOB-MRI)	0.006	0.476	0.945	0.010

PPV: positive predictive value, NPV: negative predictive value, CE-CT: contrast-enhanced computed tomography, EC-MRI: extracellular gadolinium based contrast-enhanced MRI, EOB-MRI: gadoxetic acid-enhanced MRI

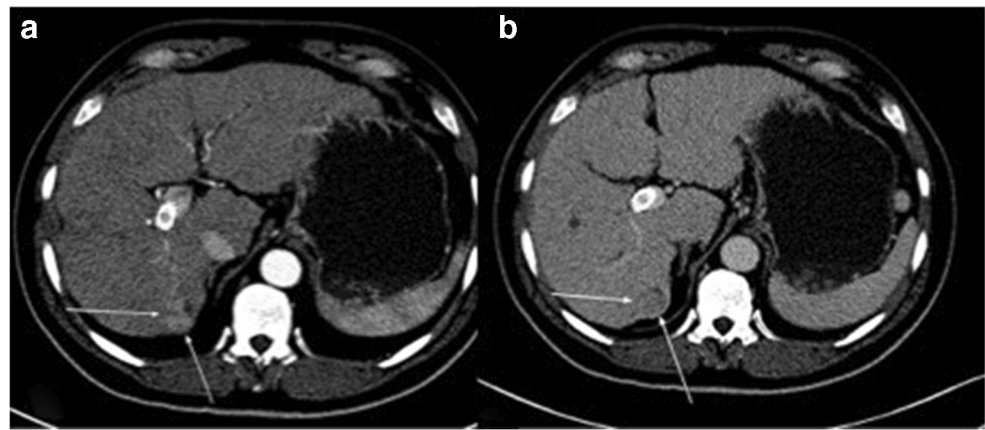
MRI and EOB-MRI groups for detection of 1–1.9 cm HCCs ( $p=0.9$  and  $0.249$ , pooled reader data, for dynamic and full EOB-MRI, respectively).

### Added value of HBP sequence

The addition of the HBP sequence obtained in the EOB-MRI dataset significantly improved per-lesion sensitivity for HCC detection (from  $69.7\%$  to  $76.8\%$ ;  $p=0.006$ ) (Table 2). Readers 1, 2 and 3 detected 12, 13 and 15

additional HCCs with the addition of HBP images, in comparison with dynamic EOB dataset, respectively (Fig. 3). This improvement was also significant for HCCs 1–1.9 cm ( $p=0.002$ ) (Table 3). Despite the improvement in HCC detection with the addition of HBP sequences, there was no significant difference with EC-MRI. All HCCs but two were hypointense on HBP; the two isointense HCCs demonstrated typical findings on dynamic imaging and were both moderately differentiated on pathology. There were no hyperintense HCCs.

**Fig. 2** 52-year-old male patient with chronic hepatitis C-related liver cirrhosis and HCC diagnosed with CT. **(a)** Axial arterial phase post-contrast image demonstrates hyperenhancement of the lesion (arrows). **(b)** Axial portal venous phase post-contrast image demonstrates lesion wash-out and capsule (arrows). Abbreviations: HCC: hepatocellular carcinoma, CT: contrast-enhanced computed tomography.



### False-positive lesions

Two FP lesions were recorded in the CT group (1 for reader 1 and 2 for reader 2, none for reader 3, mean size 15.7 mm, range: 10–18 mm). Two FP were recorded in EC-MRI group (both for reader 2, sizes: 11 and 13 mm). For the dynamic EOB-MRI group, four FP were recorded (3 for reader 1 and 1 for reader 2, none for reader 3, mean size: 15.1 mm, range 11–20 mm). For the full EOB-MRI group, two FP for each reader were recorded (mean size: 14.5 mm, range 11–18 mm). When correlating with pathology, three of the FP lesions identified represented dysplastic nodules (11, 17 and 18 mm) and the rest had no correlate on explant and were thus presumed to represent areas of shunting or posttreatment changes.

### Discussion

Our study demonstrates that EC-MRI and EOB-MRI are superior to CT for HCC detection on both per-patient and per-lesion basis, particularly for lesions 1–1.9 cm. We observed that EC-MRI was slightly superior to dynamic EOB-MRI on a per-lesion analysis, although without statistical difference between both techniques. We also observed that the addition of HBP

sequence to dynamic EOB-MRI significantly improved HCC detection, particularly for lesions 1–1.9 cm, as shown before [14]. Despite this improvement in performance, there was still no significant difference in HCC detection compared to EC-MRI. On a per-patient perspective, sensitivity of full EOB-MRI was significantly higher than that of CT and EC-MRI.

It is generally accepted that dynamic MRI has high diagnostic accuracy for HCC detection, outperforming CT, for lesions <2 cm [4, 7, 8, 24]. Regarding comparison of CT and EOB-MRI, two meta-analyses including comparative studies concluded that EOB-MRI was more sensitive for HCC detection [4, 31]. The present study is in line with these results as it shows a higher diagnostic accuracy for both MRI groups compared to CT, albeit in different populations. CT has the advantage over MRI as being more available, rapid and robust. The main disadvantages of CT are the radiation exposure and lower sensitivity for small lesions (as shown in the present study). Compared to CT, MRI provides higher contrast resolution and assessment of a greater number of tissue properties, which are valuable for lesion detection and characterization [3]. However, MRI is limited by accessibility, longer acquisition time, the need for optimization and expertise to be accurately interpreted, and increased sensitivity to motion [3].

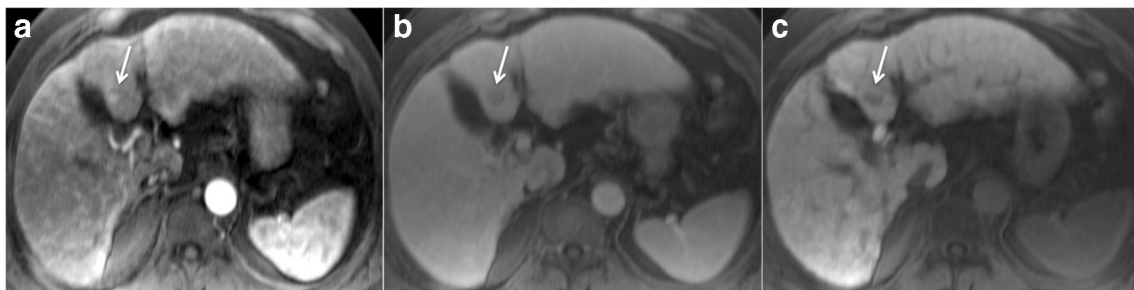


**Fig. 3** 56-year-old male patient with chronic hepatitis C-related cirrhosis and HCC, evaluated with gadoxetic acid-enhanced MRI. **(a)** Axial fat suppressed T1-weighted image obtained during the arterial phase demonstrates 1.3 cm partially hyperenhancing lesion in segment 4 (arrow) with corresponding washout at the portal venous phase **(b)**, arrow). The lesion demonstrates hypointensity on axial fat suppressed T1-weighted

image obtained at the hepatobiliary phase **(c)**, arrow). On initial evaluation, none of the readers identified the lesion on dynamic imaging, but the lesion was reclassified as LI-RADS 5 during the second reading session by all 3 readers. Abbreviations: HCC: hepatocellular carcinoma, LI-RADS: Liver Imaging Reporting and Data System.

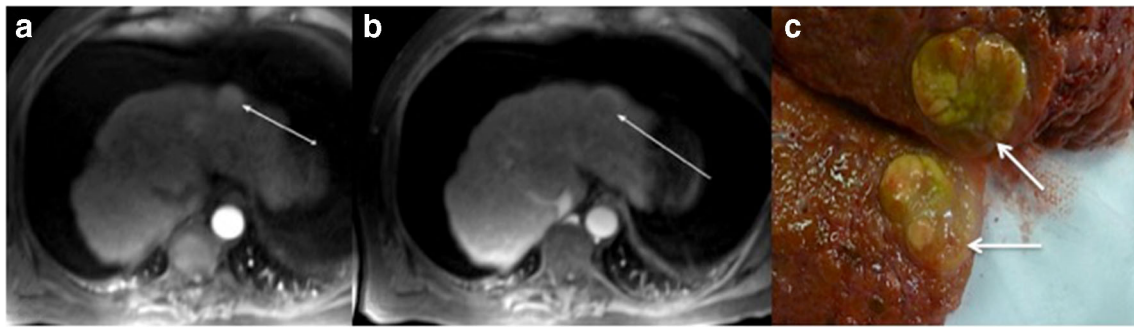


**Fig. 4** 57-year-old male patient with alcoholic liver cirrhosis and HCC, evaluated with MRI using EC-GBCA (gadobutrol). **(a)** Axial fat suppressed T1-weighted image obtained at the early arterial phase demonstrates 2.1 cm hyperenhancing lesion in segment 2 (arrow) with corresponding washout and capsule at the portal venous phase (arrow, **b**). All

three readers characterized the lesion as LI-RADS 5. **(c)** Gross section of the explanted liver demonstrates 2.2 cm HCC (arrows). Abbreviations: HCC: hepatocellular carcinoma, EC-GBCA: extracellular gadolinium based contrast agents, LI-RADS: Liver Imaging Reporting and Data System.

EOB-MRI is often presented as a viable alternative to ECCM, with the added value of HBP. However, compared to ECCM, gadoxetic acid have several limitations: 1) Higher risk of arterial phase respiratory artifact (called transient severe motion), described in up to 17% of MRI examinations with gadoxetic acid, compared to 2% with ECCM in a prospective study [32]. 2) Dynamic imaging quality is also limited due to the smaller amount of gadolinium injected (0.025 mmol/kg for Gd-EOB-DTPA compared to 0.1 mmol/kg for ECCM), counterbalanced by a higher R1 relaxivity [33]. 3) Quality of the transitional phase is limited by early hepatocyte uptake of contrast, confounding assessment of

lesion washout [34]. 4) Detection of HCC can be challenging in the setting of severe liver dysfunction, cholestasis, or biliary obstruction, in which hepatocyte contrast uptake can be significantly reduced or absent. 5) Cost of gadoxetic acid is higher compared to ECCM, in addition to the longer acquisition time. Limitations related to the dynamic phases can explain the low sensitivity for HCC detection per-lesion of dynamic EOB-MRI (69.7% with dynamic EOB-MRI, compared to 78.5% with EC-MRI, pooled reader data) in the present study, albeit not statistically different to EC-MRI. The addition of HBP has shown to improve lesion conspicuity compared to arterial phase imaging alone [25]. Additionally, the

**Table 3** Per-lesion sensitivity for each modality for HCC detection stratified by lesion size with 95% confidence intervals

	Size 1–1.9 cm				Size ≥ 2 cm			
	Reader 1	Reader 2	Reader 3	Pooled Reader Data	Reader 1	Reader 2	Reader 3	Pooled Reader Data
CT	32.8% (21.6–45.7%)	39.1% (27.1–52.1%)	31.3% (20.2–44.1%)	34.4% (27.7–41.6%)	89.6% (77.3–96.5%)	95.8% (85.8–99.5%)	93.8% (82.8–98.7%)	93.1% (87.6–96.6%)
EC-MRI	63.6% (45.1–79.6%)	63.6% (45.1–79.6%)	66.7% (48.2–82.0%)	64.6% (54.4–74.0%)	89.7% (75.8–97.1%)	92.3% (79.1–98.4%)	92.3% (79.1–98.4%)	91.5% (84.8–95.8%)
Dynamic EOB-MRI	52.0% (41.8–62.1%)	60.0% (49.7–69.7%)	60.0% (49.7–69.7%)	57.3% (51.5–63.0%)	78.2% (68.0–86.3%)	89.7% (81.3–95.2%)	83.9% (74.5–90.9%)	83.9% (78.9–88.2%)
Full EOB-MRI	61.0% (50.7–70.6%)	72.0% (62.1–80.5%)	69.0% (59.0–77.9%)	67.3% (61.7–72.6%)	81.6% (71.9–89.1%)	90.8% (82.7–96.0%)	90.8% (82.7–96.0%)	87.7% (83.1–91.5%)
<i>p</i> (CT vs. EC-MRI)	0.038	0.044	0.001	0.012	0.644	0.424	0.704	0.529
<i>p</i> (CT vs. Dynamic EOB-MRI)	0.020	0.006	< 0.001	0.001	0.426	0.755	0.638	0.491
<i>p</i> (CT vs. Full EOB-MRI)	0.002	< 0.001	0.002	0.003	0.705	0.901	0.623	0.987
<i>p</i> (EC-MRI vs. Dynamic EOB-MRI)	0.863	0.796	0.901	0.900	0.830	0.519	0.996	0.919
<i>p</i> (EC-MRI vs. Full EOB-MRI)	0.515	0.152	0.413	0.249	0.871	0.422	0.397	0.528
<i>p</i> (Dynamic EOB-MRI vs. Full EOB-MRI)	0.005	0.007	0.035	0.002	0.392	0.660	0.257	0.268

CE-CT: contrast-enhanced computed tomography, EC-MRI: extracellular gadolinium based contrast-enhanced MRI, EOB-MRI: gadoxetic acid-enhanced MRI

use of gadoxetic acid provides diagnostic information regarding both lesion characteristics and background hepatocellular function [34]. In the present study, we showed that the use of HBP allows the detection of additional lesions that are then characterized as HCC using dynamic sequences, as suggested before [21, 22, 27]. This is mainly due to increased conspicuity of HCC, which appears hypointense during HBP compared to the background liver parenchyma in over 90% of cases [25, 35]. Moreover, HBP may help differentiate benign nodules from HCC based on gadoxetic acid uptake [34]. In addition, gadoxetic acid may allow improved confidence in the evaluation and characterization of pseudolesions and peritumoral areas. The potential benefit of EOB-MRI has to be balanced with the risk of gadolinium tissue deposition in the brain when used repeatedly for surveillance that has been described to be higher with gadoxetic acid than macrocyclic GBCAs [36–38]. Future work is needed to assess the long-term effect of gadolinium deposition in tissues and investigate the risk-benefit ratio of gadoxetic acid compared to macrocyclic EC-GBCAs for HCC diagnosis. To the best of our knowledge, there is no data comparing the performance of EC-MRI to EOB-MRI using explant pathology as the reference. Kierans et al presented the lack of explant correlation as an important bias of their meta-analysis (only 13% of the selected studies included explant correlation) [39]. A small prospective crossover study from Besa et al demonstrated similar image quality for both GBCAs, with EOB-MRI being slightly superior to EC-MRI in terms of HCC detection [25]. More recently, in a prospective study in 91 patients with explant and resection specimen correlation, Min et al found that EC-MRI was superior to EOB-MRI for the diagnosis of HCC (sensitivity 77.9% vs. 66.3% for EC-MRI and EOB-MRI, respectively) [27]. The authors performed this analysis on a by-lesion perspective and explained the worse sensitivity of EOB-MRI with the known limitations of gadoxetic acid during the dynamic phase. In the present study, we found the same range of sensitivity for dynamic EOB-MRI (69.7%) but with a significant increase in lesion detection when adding HBP (76.8% for full EOB-MRI,  $p = 0.006$ ). On a per-patient basis, we showed superiority of EOB-MRI for HCC detection compared to EC-MRI and CT, which may motivate the use of abbreviated EOB-MRI for HCC screening and surveillance [40].

Using liver explant pathology as the reference standard presents the advantage of sampling the whole liver, compared to biopsy. Moreover, biopsies are limited by intra-tumoral heterogeneity that limits biopsy performance known to have a sampling error rate as high as 20.3% [41, 42]. Our results are thus not limited to a patient-level but can be extended to a lesion-level analysis. This revealed that sensitivity was lower in smaller HCC. This could be explained by lack of hypervascularity in early stage HCC [43].

There are several limitations to our study. It was a retrospective single-center study. The CT and MR systems used were different, and the time ranges in which the various modalities were used differed, which may result in varying image quality and signal-to-noise ratios. For this reason, we were not able to assess DWI, as it was not obtained in all the MRIs. The added value of DWI has already been shown, including with explant correlation [5]. The patient populations in the different groups were different, with a higher HCC prevalence and treated patients in EOB-MRI group. The patients were grouped according to the type of imaging that was performed based on the referring physician choice, inducing a possible selection bias between imaging modalities. A large crossover prospective study would be ideal, however more difficult to perform. As we excluded 5 lesions from the analysis (cholangiocarcinoma and mixed HCC-cholangiocarcinoma), we acknowledge a slight overestimation of the diagnostic performance. We believe that this effect should be limited as the total of included lesions is high (265 lesions) and as we only excluded the lesions but not the patients.

In conclusion, our study demonstrates that MRI outperforms CT in detecting HCC, particularly for lesions measuring 1–1.9 cm, without significant difference in the performance of EC-GBCAs and Gadoxetic acid. EOB-MRI outperforms EC-MRI for per-patient HCC detection, and the addition of HBP improves the detection of small HCCs.

**Funding information** The authors state that this work has not received any funding.

## Compliance with ethical standards

**Guarantor** The scientific guarantor of this publication is Bachir Taouli.

**Conflict of interest** The authors of this manuscript declare relationships with the following companies:

Bachir Taouli: Grant, Bayer Healthcare.

The other authors of this manuscript declare no relationships with any companies, whose products or services may be related to the subject matter of the article.

**Statistics and biometry** One of the authors (JS Babb) has significant statistical expertise.

**Informed consent** Written informed consent was waived by the Institutional Review Board.

**Ethical approval** Institutional Review Board approval was obtained.

## Methodology

- retrospective.
- case-control study.
- performed at one institution.

## References

- Torre LA, Bray F, Siegel RL, Ferlay J, Lortet-Tieulent J, Jemal A (2015) Global cancer statistics, 2012. *CA Cancer J Clin* 65:87–108
- Wald C, Russo MW, Heimbach JK, Hussain HK, Pomfret EA, Bruix J (2013) New OPTN/UNOS policy for liver transplant allocation: standardization of liver imaging, diagnosis, classification, and reporting of hepatocellular carcinoma. *Radiology* 266:376–382
- Choi JY, Lee JM, Sirlin CB (2014) CT and MR imaging diagnosis and staging of hepatocellular carcinoma: part II. Extracellular agents, hepatobiliary agents, and ancillary imaging features. *Radiology* 273:30–50
- Guo J, Seo Y, Ren S et al (2016) Diagnostic performance of contrast-enhanced multidetector computed tomography and gadoxetic acid disodium-enhanced magnetic resonance imaging in detecting hepatocellular carcinoma: direct comparison and a meta-analysis. *Abdom Radiol (NY)* 41:1960–1972
- Park MS, Kim S, Patel J et al (2012) Hepatocellular carcinoma: detection with diffusion-weighted versus contrast-enhanced magnetic resonance imaging in pretransplant patients. *Hepatology* 56:140–148
- Choi SH, Lee JM, Yu NC et al (2008) Hepatocellular carcinoma in liver transplantation candidates: detection with gadobenate dimeglumine-enhanced MRI. *AJR Am J Roentgenol* 191:529–536
- Baek CK, Choi JY, Kim KA et al (2012) Hepatocellular carcinoma in patients with chronic liver disease: a comparison of gadoxetic acid-enhanced MRI and multiphase MDCT. *Clin Radiol* 67:148–156
- Di Martino M, Marin D, Guerrisi A et al (2010) Intraindividual comparison of gadoxetate disodium-enhanced MR imaging and 64-section multidetector CT in the detection of hepatocellular carcinoma in patients with cirrhosis. *Radiology* 256:806–816
- Di Martino M, De Filippis G, De Santis A et al (2013) Hepatocellular carcinoma in cirrhotic patients: prospective comparison of US, CT and MR imaging. *Eur Radiol* 23:887–896
- Libbrecht L, Bielen D, Verslype C et al (2002) Focal lesions in cirrhotic explant livers: pathological evaluation and accuracy of pretransplantation imaging examinations. *Liver Transpl* 8:749–761
- Junqiang L, Yinzhong W, Li Z et al (2014) Gadoxetic acid disodium (Gd-EOBDTPA)-enhanced magnetic resonance imaging for the detection of hepatocellular carcinoma: a meta-analysis. *J Magn Reson Imaging* 39:1079–1087
- Akai H, Kiryu S, Matsuda I et al (2011) Detection of hepatocellular carcinoma by Gd-EOB-DTPA-enhanced liver MRI: comparison with triple phase 64 detector row helical CT. *Eur J Radiol* 80:310–315
- Ichikawa T, Saito K, Yoshioka N et al (2010) Detection and characterization of focal liver lesions: a Japanese phase III, multicenter comparison between gadoxetic acid disodium-enhanced magnetic resonance imaging and contrast-enhanced computed tomography predominantly in patients with hepatocellular carcinoma and chronic liver disease. *Invest Radiol* 45:133–141
- Park MJ, Kim YK, Lee MW et al (2012) Small hepatocellular carcinomas: improved sensitivity by combining gadoxetic acid-enhanced and diffusion-weighted MR imaging patterns. *Radiology* 264:761–770
- Hwang J, Kim YK, Kim JM, Lee WJ, Choi D, Hong SS (2014) Pretransplant diagnosis of hepatocellular carcinoma by gadoxetic acid-enhanced and diffusion-weighted magnetic resonance imaging. *Liver Transpl* 20:1436–1446
- Cortis K, Liotta R, Miraglia R, Caruso S, Tuzzolino F, Luca A (2016) Incorporating the hepatobiliary phase of gadobenate dimeglumine-enhanced MRI in the diagnosis of hepatocellular carcinoma: increasing the sensitivity without compromising specificity. *Acta Radiol* 57:923–931
- Luca A, Caruso S, Milazzo M et al (2010) Multidetector-row computed tomography (MDCT) for the diagnosis of hepatocellular carcinoma in cirrhotic candidates for liver transplantation: prevalence of radiological vascular patterns and histological correlation with liver explants. *Eur Radiol* 20:898–907
- Maetani YS, Ueda M, Haga H et al (2008) Hepatocellular carcinoma in patients undergoing living-donor liver transplantation. Accuracy of multidetector computed tomography by viewing images on digital monitors. *Intervirology* 51(Suppl 1):46–51
- Becker-Weidman DJ, Kalb B, Sharma P et al (2011) Hepatocellular carcinoma lesion characterization: single-institution clinical performance review of multiphase gadolinium-enhanced MR imaging—comparison to prior same-center results after MR systems improvements. *Radiology* 261:824–833
- Lauenstein TC, Salman K, Morreira R et al (2007) Gadolinium-enhanced MRI for tumor surveillance before liver transplantation: center-based experience. *AJR Am J Roentgenol* 189:663–670
- Orlacchio A, Chegai F, Fabiano S et al (2016) Role of MRI with hepatospecific contrast agent in the identification and characterization of focal liver lesions: pathological correlation in explanted livers. *Radiol Med* 121:588–596
- Lee DH, Lee JM, Baek JH, Shin CI, Han JK, Choi BI (2015) Diagnostic performance of gadoxetic acid-enhanced liver MR imaging in the detection of HCCs and allocation of transplant recipients on the basis of the Milan criteria and UNOS guidelines: correlation with histopathologic findings. *Radiology* 274:149–160
- Bartolozzi C, Battaglia V, Bargellini I et al (2013) Contrast-enhanced magnetic resonance imaging of 102 nodules in cirrhosis: correlation with histological findings on explanted livers. *Abdom Imaging* 38:290–296
- Burrell M, Llovet JM, Ayuso C et al (2003) MRI angiography is superior to helical CT for detection of HCC prior to liver transplantation: an explant correlation. *Hepatology* 38:1034–1042
- Besa C, Kakite S, Cooper N, Facciuto M, Taouli B (2015) Comparison of gadoxetic acid and gadopentetate dimeglumine-enhanced MRI for HCC detection: prospective crossover study at 3 T. *Acta Radiol Open* 4:2047981614561285
- Ahn SS, Kim MJ, Lim JS, Hong HS, Chung YE, Choi JY (2010) Added value of gadoxetic acid-enhanced hepatobiliary phase MR imaging in the diagnosis of hepatocellular carcinoma. *Radiology* 255:459–466
- Min JH, Kim JM, Kim YK et al (2018) Prospective Intraindividual comparison of MRI with Gadoxetic acid and extracellular contrast for diagnosis of HCCs using LI-RADS. *Hepatology*. <https://doi.org/10.1002/hep.30122>
- Bruix J, Sherman M, American Association for the Study of Liver Diseases (2011) Management of hepatocellular carcinoma: an update. *Hepatology* 53:1020–1022
- European Association for the Study of the Liver (2018) EASL clinical practice guidelines: management of hepatocellular carcinoma. *J Hepatol* 69:182–236
- LIRADS\_2017\_CORE. Available via [https://www.acr.org/-/media/ACR/Files/RADS/LI-RADS/LIRADS\\_2017\\_Core.pdf?la=en](https://www.acr.org/-/media/ACR/Files/RADS/LI-RADS/LIRADS_2017_Core.pdf?la=en)
- Roberts LR, Sirlin CB, Zaiem F et al (2018) Imaging for the diagnosis of hepatocellular carcinoma: a systematic review and meta-analysis. *Hepatology* 67:401–421
- Davenport MS, Vigiante BL, Al-Hawary MM et al (2013) Comparison of acute transient dyspnea after intravenous administration of gadoxetate disodium and gadobenate dimeglumine: effect on arterial phase image quality. *Radiology* 266:452–461
- Tanimoto A, Higuchi N, Ueno A (2012) Reduction of ringing artifacts in the arterial phase of gadoxetic acid-enhanced dynamic MR imaging. *Magn Reson Med Sci* 11:91–97
- Cruite I, Schroeder M, Merkle EM, Sirlin CB (2010) Gadoxetate disodium-enhanced MRI of the liver: part 2, protocol optimization

- and lesion appearance in the cirrhotic liver. *AJR Am J Roentgenol* 195:29–41
35. Kitao A, Zen Y, Matsui O et al (2010) Hepatocellular carcinoma: signal intensity at gadoxetic acid-enhanced MR imaging—correlation with molecular transporters and histopathologic features. *Radiology* 256:817–826
  36. Kahn J, Posch H, Steffen IG et al (2017) Is there long-term signal intensity increase in the central nervous system on T1-weighted images after MR imaging with the Hepatospecific contrast agent Gadoxetic acid? A cross-sectional study in 91 patients. *Radiology* 282:708–716
  37. Radbruch A, Weberling LD, Kieslich PJ et al (2015) Gadolinium retention in the dentate nucleus and globus pallidus is dependent on the class of contrast agent. *Radiology* 275:783–791
  38. Radbruch A, Weberling LD, Kieslich PJ et al (2015) High-signal intensity in the dentate nucleus and Globus pallidus on unenhanced T1-weighted images: evaluation of the macrocyclic gadolinium-based contrast agent Gadobutrol. *Invest Radiol* 50:805–810
  39. Kierans AS, Kang SK, Rosenkrantz AB (2016) The diagnostic performance of dynamic contrast-enhanced MR imaging for detection of small hepatocellular carcinoma measuring up to 2 cm: a meta-analysis. *Radiology* 278:82–94
  40. Besa C, Lewis S, Pandharipande PV et al (2017) Hepatocellular carcinoma detection: diagnostic performance of a simulated abbreviated MRI protocol combining diffusion-weighted and T1-weighted imaging at the delayed phase post gadoxetic acid. *Abdom Radiol (NY)* 42:179–190
  41. Claudon M, Dietrich CF, Choi BI et al (2013) Guidelines and good clinical practice recommendations for contrast enhanced ultrasound (CEUS) in the liver - update 2012: a WFUMB-EFSUMB initiative in cooperation with representatives of AFSUMB, AIUM, ASUM, FLAUS and ICUS. *Ultrasound Med Biol* 39:187–210
  42. Robert M, Sofair AN, Thomas A et al (2009) A comparison of hepatopathologists' and community pathologists' review of liver biopsy specimens from patients with hepatitis C. *Clin Gastroenterol Hepatol* 7:335–338
  43. International Consensus Group for Hepatocellular NeoplasiaThe International Consensus Group for Hepatocellular Neoplasia (2009) Pathologic diagnosis of early hepatocellular carcinoma: a report of the international consensus group for hepatocellular neoplasia. *Hepatology* 49:658–664

**Publisher's note** Springer Nature remains neutral with regard to jurisdictional claims in published maps and institutional affiliations.